Design Aspects of Coils for EDS Levitation Systems

M. Andriollo
Dipartimento di Ingegneria Elettrica, Università degli Studi di Padova, Padova, Italy
T. Bertoncelli[1], F. Castelli Dezza, D. Rosati
Dipartimento di Elettrotecnica, Politecnico di Milano, Milano, Italy

[1] *presently at Max-Planck-Institut für Plasmaphysik, Garching (Germany), tiziana.bertoncelli@ipp.mpg.de*

ABSTRACT: EDS systems based on high frequency supplied windings are convenient candidates in standstill and low motion applications where strict mechanical tolerances are not practicable. In this paper a simple EDS system, based on a single levitation coil, is analyzed by an implementation of analytical formulations of the levitation force and of the vertical levitation stiffness. Such methodology can be effective for the parametric analysis to investigate the influence of the geometric sizes and to optimize the system performance taking into account the design constraints.

1 INTRODUCTION

In some industrial application magnetic levitation may be a desirable option, provided that it is achieved with a relatively inexpensive apparatus, using robust control system, and when mechanical tolerances are not too severe. To such purpose, EDS systems based on high frequency supplied windings can be convenient candidates, especially in standstill and low motion applications, since levitation is independent from the relative motion between the load and the active or passive guideway. In its simplest configuration, an EDS levitation system is represented by a coil faced to an horizontal slab with high electrical conductivity σ and magnetic permeability $\mu \approx \mu_0$ (Fig. 1), Thompson (2000). Supplying the coil with an alternating current of relatively high frequency f and provided that the conducting plate thickness is larger than the penetration depth $\delta = 1/\sqrt{\pi f \mu \sigma}$, the electrodynamic effect can be reproduced by replacing the plate itself with a fictitious "image" coil placed symmetrically to the real coil with respect to the plate surface (Fig. 2). The main drawback of this arrangement is represented by the sizing of the coil supply system, especially taking into account that most of the absorbed power is represented by the reactive component. In the variable frequency supply system investigated by the authors, the reactive power is compensated by a parallel connected capacitor bank, allowing to operate near the anti-resonance condition.

From the application point of view, the reversed arrangement levitating sheet–fixed coil could be even more attractive, provided that the sheet weight is not excessive, nevertheless it can be analyzed exactly with the same approach. The results and the experimental setup described in this paper refers anyway to the configuration with a levitating coil.

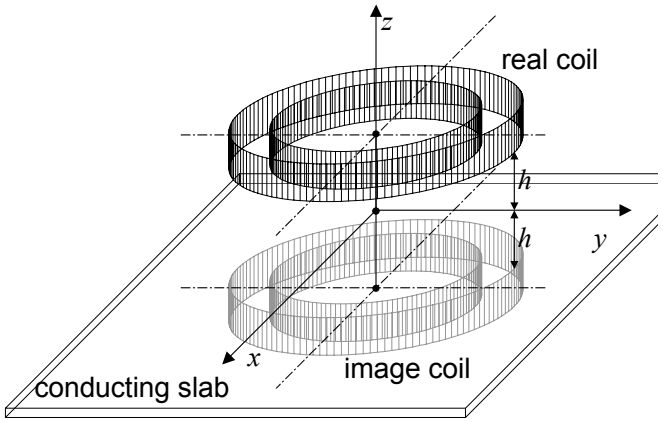

Figure 1: Axonometric view of the coil and of its mirror image (*h*: levitation height)

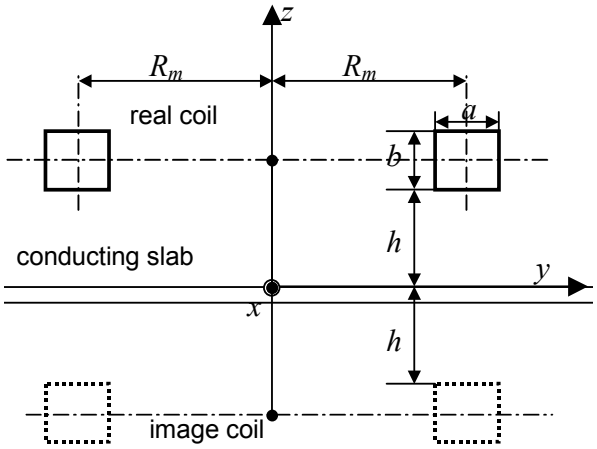

Figure 2: Coil sizes (*a*, *b*: cross section width and height, R_m: mean coil radius).

2 ANALYTICAL FORMULATIONS

As a preliminary hypothesis, the plate faced to the coil is assumed to be made of a perfectly conducting materials, so that the image principle is exactly applicable. Many analytical and pseudo-analytical formulations related to such configuration can be retrieved in literature, mainly concerned with the evaluation of coil self and mutual inductances. The electrodynamic effects can be derived from such formulations taking the derivative of the magnetic energy with respect to the displacement variable or by the direct integration of the expression of Lorentz' force all over the coils volume. Nevertheless the implementation of these approaches could result fairly onerous from the computational point of view, if a good accuracy is required for a wide range of coils configurations. An effective calculation procedure can be particularly convenient when the influence of the geometric sizes has to be investigated via a parametric analysis, in order to optimize the system performance taking into account the design constraints. A shortcut for the calculation of the levitation force can be obtained by applying the virtual work principle, taking into account that a vertical coil displacement *dz* results in an opposite displacement *–dz* of the image coil, so the relative displacement is 2*dz* (Fig.3). According to this figure, the variation of magnetic energy due to the infinitesimal vertical displacement 2*dz* can be obtained as twice the difference between the values of the surface integral of the tangential component $A_\theta(r,z)$ of the magnetic potential vector generated by the image coil on the upper and on the lower face of the coil, i.e.:

$$dW_m = -F_z(h)dz = \frac{1}{2}\cdot 2dzJ\cdot \int_{R_m-\frac{a}{2}}^{R_m+\frac{a}{2}}\left(A_\theta\left(r,2h+\frac{3b}{2}\right)-A_\theta\left(r,2h+\frac{b}{2}\right)\right)2\pi r dr \quad (1)$$

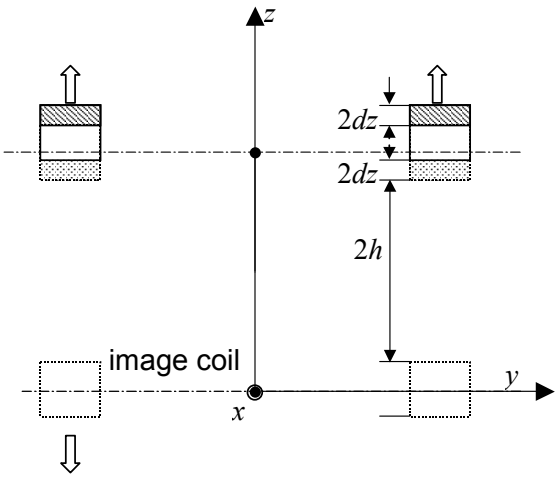

Figure 3: Application of the virtual work principle related to a vertical displacement *dz* to evaluate the levitation force F_z.

where J is the current density and $A_\theta(r,z)$ is expressed according to a reference frame with the origin placed in the centre of the image coil by the volume integral:

$$A_\theta(r,z)=\frac{\mu_0 J}{2\pi}\int_0^{\pi}\int_{R_m-\frac{a}{2}}^{R_m+\frac{a}{2}}\int_{-\frac{b}{2}}^{\frac{b}{2}}\frac{\rho\cos\theta\cdot d\theta\cdot d\rho\cdot d\zeta}{\sqrt{(r-\rho)^2+(z-\zeta)^2-2r\rho\cos\theta}} \quad (2)$$

The evaluation of (2) can involve the routines for the calculation of the well-known complete integrals of the first and of the second kind K and E. It is also possible to use expressions based on the analytical formulations of the mutual inductance between a thin-wall solenoid and a disk coil, Babic & Akyel (2000). It is convenient to adopt a per unit notation assuming the levitation height h as the basis quantity and denoting by the * superscript the per unit values. The levitation force can be therefore expressed as:

$$F_z(h)=2\pi J^2 h^4\int_{R_m^*-\frac{a^*}{2}}^{R_m^*+\frac{a^*}{2}}\left(a_\theta^*\left(r^*,2+\frac{b^*}{2}\right)-a_\theta^*\left(r^*,2+\frac{3b^*}{2}\right)\right)r^* dr^* \quad (3)$$

where the function with dimensionless arguments:

$$a_\theta^*(r^*,z^*)=\frac{\mu_0}{2\pi}\cdot \int_0^{\pi}\int_{R_m^*-\frac{a^*}{2}}^{R_m^*+\frac{a^*}{2}}\int_{-\frac{b^*}{2}}^{\frac{b^*}{2}}\frac{\rho^*\cos\theta\cdot d\theta\cdot d\rho^*\cdot d\zeta^*}{\sqrt{(r^*-\rho^*)^2+(z^*-\zeta^*)^2-2r^*\rho^*\cos\theta}} \quad (4)$$

doesn't depend on the system scale but only on the size proportions. Therefore (4) evidences that the force grows with the power of four with respect to the system linear size, the same current density being maintained, according to a well-known law scale.

The integration of (4) first with respect to ζ^* and then with respect to θ yields the formulation:

$$a_\theta^*(r^*,z^*)=\frac{\mu_0}{2\pi}\int_{R_m^*-\frac{a^*}{2}}^{R_m^*+\frac{a^*}{2}}\rho^*\left(g\left(4\left(r^{*2}+\rho^{*2}\right),8r^*\rho^*,2z^*+b^*\right)-g\left(4\left(r^{*2}+\rho^{*2}\right),8r^*\rho^*,2z^*-b^*\right)\right)d\rho^* \quad (5)$$

with:

$$g(\chi_1,\chi_2,\chi_3)=$$
$$=\frac{1}{2\chi_2}\left(-\pi\left(\chi_1-\sqrt{\chi_1^2-\chi_2^2}\right)+\frac{2\chi_3}{\sqrt{\chi_1+\chi_2+\chi_3^2}}\cdot\right.$$
$$\cdot\left(\left(\chi_2-\chi_1\right)\Pi\left(\frac{2\chi_2}{\chi_1+\chi_2},\frac{2\chi_2}{\chi_1+\chi_2+\chi_3^2}\right)-\left(\chi_1+\chi_2+\chi_3^2\right)\cdot\right. \quad (6)$$
$$\left.\left.\cdot E\left(\frac{2\chi_2}{\chi_1+\chi_2+\chi_3^2}\right)+\left(2\chi_1+\chi_3^2\right)K\left(\frac{2\chi_2}{\chi_1+\chi_2+\chi_3^2}\right)\right)\right)$$

where K, E and Π are the complete elliptic integrals of the first, second and third kind, respectively.

The average levitation force/coil volume ratio ϕ can be adopted as a performance index, and can be expressed as:

$$\phi=\frac{\langle F_z(h)\rangle}{2\pi R_m ab}=\frac{J_{rms}^2 h}{R_m^* a^* b^*}\cdot$$
$$\cdot\int_{R_m^*-\frac{a^*}{2}}^{R_m^*+\frac{a^*}{2}}\left(a_\theta^*\left(r^*,2+\frac{b^*}{2}\right)-a_\theta^*\left(r^*,2+\frac{3b^*}{2}\right)\right)r^*dr^* \quad (7)$$

Therefore the performance improves proportionally to the system scale since ϕ varies linearly with h, the same geometric proportions being maintained. As regards the dynamic behaviour, the vertical stiffness $S_z=\partial F_z/\partial z$ is a fundamental parameter to define the angular frequency of the undamped oscillations; according to (3), (4) and (5), S_z can be obtained as:

$$S_z=\frac{\partial F_z}{\partial z}=2\pi\mu_0 J^2 h^3\cdot$$
$$\cdot\int_{R_m^*-\frac{a^*}{2}}^{R_m^*+\frac{a^*}{2}}\left(k_\theta^*\left(r^*,2+\frac{b^*}{2}\right)-k_\theta^*\left(r^*,2+\frac{3b^*}{2}\right)\right)r^*dr^* \quad (8)$$

where:

$$k_\theta^*\left(r^*,z^*\right)=\frac{\mu_0}{2\pi}\cdot$$
$$\cdot\int_{R_m^*-\frac{a^*}{2}}^{R_m^*+\frac{a^*}{2}}\rho^*\left(m\left(r^{*2}+\rho^{*2}+\left(z^*-\frac{b^*}{2}\right),2r^*\rho^*\right)-\right. \quad (9)$$
$$\left.-m\left(r^{*2}+\rho^{*2}+\left(z^*+\frac{b^*}{2}\right),2r^*\rho^*\right)\right)d\rho^*$$

with:

$$m(\chi_1,\chi_2)=2\frac{(\chi_1+\chi_2)E\left(\frac{2\chi_2}{\chi_1+\chi_2}\right)-\chi_1 K\left(\frac{2\chi_2}{\chi_1+\chi_2}\right)}{\chi_2\sqrt{\chi_1+\chi_2}} \quad (10)$$

It's worth to remark that, according to the formulations (3), (5), (8) and (9), only a double numerical integration with respect to the dimensionless radial coordinates r^* and ρ^* is needed to evaluate F_z and S_z, instead of the double volume integration required by the crude application of the principle of the energy variation.

3 PARAMETRICAL ANALYSIS

The implementation of the above presented formulations allow a quick analysis of the system performances as functions of the geometrical sizes. In particular, the dependence of the performance index ϕ defined in (7) on the cross section aspect ratio a/b was investigated for different values of the per unit coil average radius $R^*_m=R_m/h$, the same cross section area being maintained. It can be recognized that, for $R^*_m\to\infty$, the function ϕ approaches to the finite value ϕ_∞ represented by the force/volume ratio of an infinite length straight bar with the same cross section and levitation height. It's therefore convenient to normalize ϕ with respect to ϕ_∞. The Figure 4 allows to identify the optimal aspect ratio of the coil cross, for different values of the coil radius.

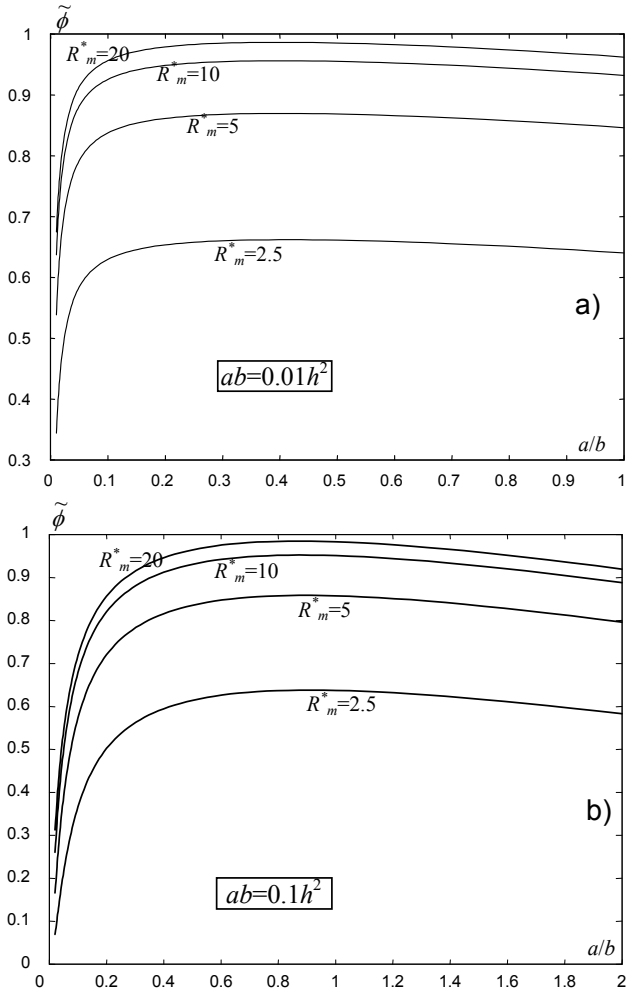

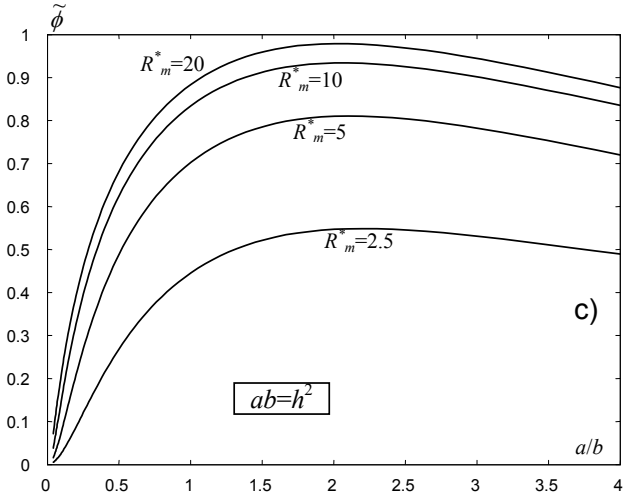

Figure 4: Normalized value of ϕ as a function of a/b for different values of R^*_m a) $a \cdot b=0.01h^2$; b) $a \cdot b=0.1h^2$; c) $a \cdot b=h^2$

It can be recognized that the variation of the cross section area remarkably affects the optimal aspect ratio and that the radius, on the contrary, has a slight influence on this quantity.

4 APPLICATION TO A TESTING SETUP

An experimental set-up was carried out for a preliminary feasibility test and allowed to check the model parameters (Andriollo et al., 2006). The test configuration includes (Figures 5, 6 and Table 1):

- a square voltage single phase inverter with an open loop voltage and frequency control;
- an output filter inductance;
- a capacitor bank, tuned to obtain a near-resonance condition with the coil inductance.

As concerns the coil, its parameters are reported in Table 2.

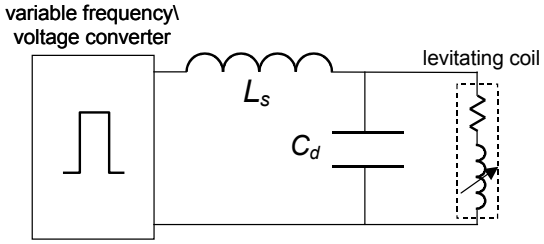

Fig. 5: Circuit diagram of the supply system.

Table 1: Experimental Set-up Parameters

Description	Value
Inverter frequency range	0 – 5 kHz
Inverter voltage range	0 – 400 V
Inverter rated current	20 A
Coil rms current density	5.32 A/mm^2
Filter Inductance L_s	0.512 mH
Bank capacitance C_d	77 μF

Table 2: Coil Parameters

Symbol	Description	Value
n	Number of turns	52
m	Coil mass	2.82 kg
R	20°C mean resistance	0.252 Ω
R_m	Mean coil radius	70 mm
a	Coil cross-section width	40 mm
b	Coil cross-section height	16 mm

With a levitation height h=7 mm, the average value of the levitation force obtained by (3) is about 11.85 N. According to the data of Table 2, the per unit volume is ≈820.7. The expression (3) as a function of a^*, b^* and R^*_m, the same volume and current density being maintained, was optimised in the Mathematica® environment: 75 configuration were considered in about 75 s (Fig.7). In the optimized configuration (Fig.8, R_m=50.94 mm, a=52.73 mm, b=16.68 mm) the levitation force is about 12.53 N (≈6% increase). An almost perfect agreement with the results of eddy current FEM simulations (relative difference less than $2 \cdot 10^{-4}$) was verified for both the actual and the optimized configurations.

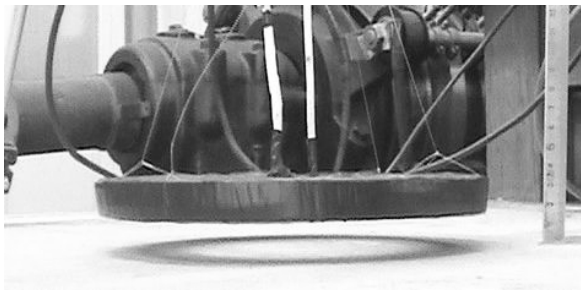

Figure 6: Experimental coil: a) Force gauge b) wire details

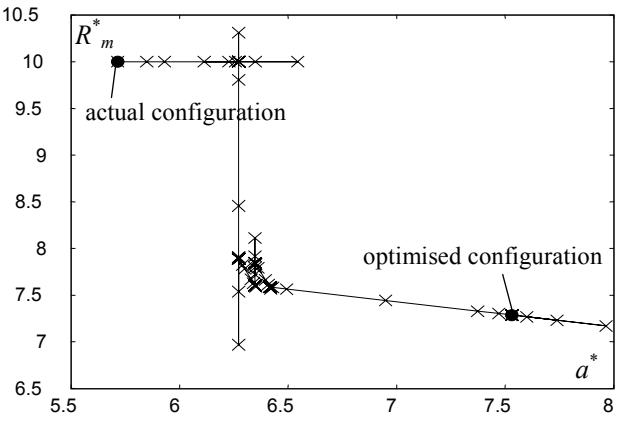

Figure 7: Progress of the optimization procedure.

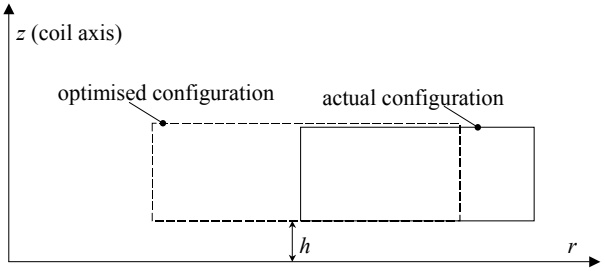

Figure 8: Configurations of the actual and of the optimized coils.

5 CONCLUSIONS

The formulations reported in this paper allow a fast evaluation of the performance (levitation force and vertical stiffness) of an EDS levitation system based on induced currents in a conducting plate by a high-frequency supplied coil. They help to identify the optimal coil configurations, taking into account various design constraints and allowing a remarkable spare of calculation time. Their exactness is confirmed by the comparison with the results of the FEM analyses.

REFERENCES

Thompson, M.T. 2000. Electrodynamic magnetic suspension – Models, scaling laws and experimental results, *IEEE Trans. on Education, vol. 43, n. 3, August 2000*: pp. 336-341.

Babic, S. & Akyel, C. 2000. Improvement in calculation of the self- and mutual inductance of thin-wall solenoids and disk coils, *IEEE Trans. on Magn., vol. 36, n. 4, July 2000*: pp. 1970-1975.

Andriollo, M., Carmeli, S., Castelli Dezza, F., Mauri, M. 2006. Control design aspects for an EDS levitation system, *Speedam Symposium, Taormina (Italy) 3-26 May 2006*, N. 31344